NASA
Technical
Paper
2182

August 1983

Solar-Simulator-Pumped Atomic Iodine Laser Kinetics

John W. Wilson,
S. Raju,
and Y. J. Shiu

NASA

25th Anniversary
1958-1983

NASA
Technical
Paper
2182

1983

Solar-Simulator-Pumped Atomic Iodine Laser Kinetics

John W. Wilson
Langley Research Center
Hampton, Virginia

S. Raju and
Y. J. Shiu
Hampton Institute
Hampton, Virginia

National Aeronautics
and Space Administration

**Scientific and Technical
Information Branch**

INTRODUCTION

High power lasers have potential in space power transmission and spacecraft propulsion. Of the several options for the generation of laser beams in space, the direct conversion of solar radiant energy into a population inversion appears particularly attractive. Direct solar pumping for space power applications was first demonstrated in alkyliodide gases. To develop this photochemical laser system further, some attention must be given to the chemical reversibility and reprocessing requirements in scaling to large space systems.

Although the photochemical processes of alkyliodide gases have been greatly clarified in recent years, considerable uncertainty in specific rate coefficients adversely impact models used for scaling of the photodissociative 1.3-μm iodine laser system (ref. 1). Through laser kinetics, the characteristic output of an experimental laser can be related to specific rate coefficients. In this way, critical coefficients can be identified and perhaps estimated from experimental lasing of the iodine atom. The laser experiments to be analyzed in this paper were performed using $n\text{-}C_3F_7I$ as the lasant, a high-pressure xenon arc lamp with a parabolic reflector as a solar simulator, and a MgF_2-coated aluminum conic collector to focus the light in the laser tube. The experimental apparatus and procedures are described in reference 2.

A preliminary model of the iodine laser kinetics (ref. 1) has shown some success in predicting the experimental laser characteristics (ref. 2), especially the lasing threshold and the early pulse structure of the laser output. The model developed in the present paper accounts for nonuniform light exposure in the laser tube and results in a reevaluation of some kinetic coefficients.

SOLAR-SIMULATOR LAMP

At the temporal peak of the solar-simulator pulse, the intensity of illumination in the region of the laser tube is

$$C(r,\ell) = C_o \exp\left[-2.77\left(\frac{\ell^2}{L^2} + \frac{r^2}{R^2}\right)\right] \tag{1}$$

where $C_o = 2.7$ kW/cm^2, $L = 4.75$ cm, $R = 0.325$ cm, ℓ is the distance along the axis of symmetry of the lamp image, and r is the corresponding radial distance. (Symbols used in this paper are defined after the references.) Because of the relatively large magnification factors in focusing the small high-pressure arc image in the laser tube, small temporal fluctuations of the arc plasma cause large spatial movements of the image in the laser tube. This produces some difficulty in interpretation of the experiments since the instantaneous pump power in the laser tube is generally less than its maximum. Only by considering many experimental runs can the ideal experimental result be identified. The photodissociation rates of the laser

gases calculated for the line width D_o and absorption cross section σ_o at the line center λ_o are

$$\xi_i = S_i[f \exp(-\sigma_o px) + (1 - f) \exp(-0.223\sigma_o px)] \quad (2)$$

where p is the alkyliodide partial pressure, x is the depth of penetration, S_i is the maximum photodissociation rate, f is the fractional absorption for wavelengths near the line center, and $(1 - f)$ is the fractional absorption in the wings. Equation (2) does not explicitly depend on line width D_o because the line width is small compared with the spectral band of the simulator output. Values of photodissociation parameters from references 3 to 5 are given in table I. The

TABLE I.- PHOTODISSOCIATION PARAMETERS USED FOR THE EQUIVALENT POWER OF ONE SOLAR CONSTANT EXPOSURE, 1.4 kW/m^2

	$n\text{-}C_3F_7I$	$i\text{-}C_3F_7I$	I_2
σ_o, cm^2	[a] 7.9×10^{-19}	[b] 6.2×10^{-19}	[c] 9.14×10^{-19}
λ_o, nm	[a] 272	[b] 275	[c] 499
D_o, nm	[a] 12.7	[b] 14.5	[c] 23.0
ϕ_{I^*}	[a] 1.0	[b] 1.0	0.51
S, s^{-1}	3.04×10^{-3}	3.37×10^{-3}	3.38×10^{-2}
f	0.652	0.653	0.673

[a]Reference 3.
[b]Reference 4.
[c]Reference 5.

effective arc temperature after reflection from the parabolic mirror was taken as 6000 K, and the reflection coefficients of the conic collector for ultraviolet (R_{uv}) and visible (R_{vis}) light are taken as those typical for MgF_2-coated aluminum surfaces.

LASER KINETICS

The basic kinetic processes for the photodissociative iodine laser are shown in figure 1 including all known chemical reactions. The kinetic equations on the center line of the 0.35-cm-radius laser tube are

$$\frac{d[RI]}{dt} = K_1[R][I^*] + K_2[R][I] - \left(\frac{R_{uv}}{R_{vis}}\right)\xi_1[RI] \tag{3}$$

$$\frac{d[R]}{dt} = \left(\frac{R_{uv}}{R_{vis}}\right)\xi_1[RI] - K_1[R][I^*] - K_2[R][I] - 2K_3[R]^2 \tag{4}$$

$$\frac{d[R_2]}{dt} = K_3[R]^2 \tag{5}$$

$$\frac{d[I_2]}{dt} = C_1[I][I^*][RI] + C_2[I]^2[RI] + C_3[I][I^*][I_2] + C_4[I]^2[I_2] - \xi_2[I_2] \tag{6}$$

$$\frac{d[I^*]}{dt} = \left(\frac{R_{uv}}{R_{vis}}\right)\xi_1[RI] + \xi_2[I_2] - K_1[R][I^*] - C_1[I][I^*][RI] - C_3[I][I^*][I_2] - Q_1[I^*][RI] - Q_2[I^*][I_2] - \Gamma_{max} - A[I^*] \tag{7}$$

$$\frac{d[I]}{dt} = \xi_2[I_2] + Q_1[I^*][RI] + Q_2[I^*][I_2] + \Gamma_{max} + A[I^*] - C_1[I][I^*][RI] - 2C_2[I]^2[RI] - C_3[I][I^*][I_2] - 2C_4[I]^2[I_2] - K_2[R][I] \tag{8}$$

$$\frac{d\rho}{dt} = \Gamma_{max}\left(\frac{\pi}{2.77}\right)^{1/2}\frac{L}{L_c} - \frac{1}{\tau_c}\rho + gA[I^*] \tag{9}$$

$$\Gamma_{max} = c\sigma\rho\left([I^*] - \frac{1}{2}[I]\right) \tag{10}$$

Kinetic rate coefficients (refs. 6 to 21) are given in table II. The stimulated emission cross section (cm^2) is (ref. 13)

$$\sigma \approx (2 \times 10^{17} + 0.443[RI])^{-1} \tag{11}$$

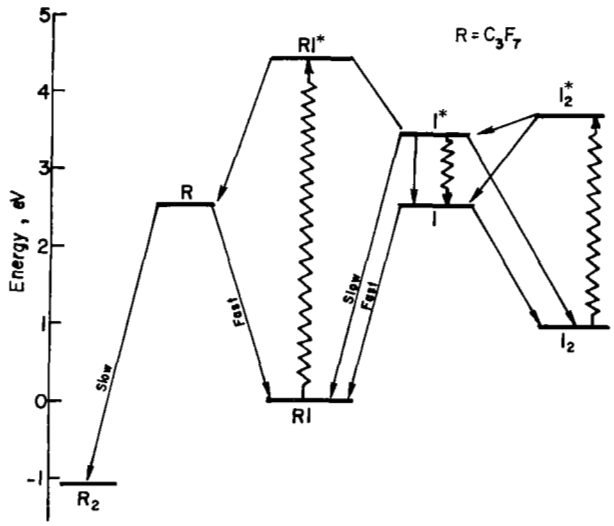

Figure 1.- Energy diagram of alkyliodide photochemical laser showing kinetic pathways.

TABLE II. - MEAN KINETIC RATE COEFFICIENTS OBTAINED FROM THE LITERATURE AND THE ASSOCIATED UNCERTAINTY FACTORS

[The factor in parentheses gives the uncertainty limits associated with each rate]

	$n\text{-}C_3F_7I$	$i\text{-}C_3F_7I$	References
K_1, cm^3/s	7.9×10^{-13} $(5.9)^{\pm1}$	4.4×10^{-13} $(5.4)^{\pm1}$	6-10
K_2, cm^3/s	2.3×10^{-11} $(3.5)^{\pm1}$	3.9×10^{-11} $(4.3)^{\pm1}$	6-11
K_3, cm^3/s	2.6×10^{-12} $(4)^{\pm1}$	9.0×10^{-13} $(3.8)^{\pm1}$	6-12
Q_1, cm^3/s	2.0×10^{-16} $(4.2)^{\pm1}$	2.8×10^{-16}	6, 7, 13, 14
Q_2, cm^3/s	1.9×10^{-11} $(2.6)^{\pm1}$	1.9×10^{-11} $(2.6)^{\pm1}$	6, 8, 12, 13, 15-19
C_1, cm^6/s	1×10^{-33}	8.8×10^{-33} $(1.2)^{\pm1}$	6, 8, 14
C_2, cm^6/s	8.5×10^{-32} $(5.3)^{\pm1}$	8.3×10^{-32} $(5.3)^{\pm1}$	6-8
C_3, cm^6/s	5.6×10^{-32} $(1.5)^{\pm1}$	5.6×10^{-32} $(1.5)^{\pm1}$	6, 8
C_4, cm^6/s	2.0×10^{-30} $(4.3)^{\pm1}$	2.0×10^{-30} $(4.3)^{\pm1}$	6, 8, 17, 20, 21

The Einstein coefficient A is 7.7 sec^{-1} (according to ref. 13), and τ_c, the optical cavity time constant (ref. 22), is

$$\tau_c = \frac{-2(L_c/c)}{\ln r_1 r_2} \tag{12}$$

where L_c is the distance (56 cm) between the mirrors forming the optical cavity, c is the velocity of light, r_1 and r_2 are the reflection coefficients (0.9775 and 0.9975) at the ends of the cavity including Brewster window losses, ρ is the average photon density in the optical cavity, and g is the coupling parameter of the spontaneous emission to the optical cavity (ref. 1):

$$g \approx \frac{2r_b^2}{L_c^2} \tag{13}$$

where r_b is the laser beam width (approximately 0.18 cm) of the appropriate oscillator mode. The factor $(\pi/2.77)^{1/2}$ in equation (9) is a geometric factor resulting from nonuniform pumping and Γ_{max} is the stimulated emission rate at the spatial peak of the pump pulse. In the above equations, the relaxation of the hyperfine states which is important in determining threshold (ref. 13) and in influencing the laser pulsations early in the laser pulse has been ignored. Special attention is now given to the quasi-CW (continuous wave) portion of the pulse for which the hyperfine relaxation times are short compared with laser pulse fluctuations. Of interest here are the kinetic processes which dominate at late times in the laser output.

After the initial laser pulsations, the photon density becomes steady as gains and losses balance each other within the cavity and gain medium, as expressed by

$$\rho = \left(\frac{\pi}{2.77}\right)^{1/2} \Gamma_{max} L \frac{\tau_c}{L_c} \tag{14}$$

or equivalently

$$[I^*] - \frac{1}{2}[I] = -\frac{1}{2} \frac{\ln r_1 r_2}{(\pi/2.77)^{1/2}} L\sigma \equiv I_{th} \tag{15}$$

where I_{th} is the threshold inversion density. One may also show that under quasi-steady-state conditions,

$$\Gamma_{max} = \left(\frac{R_{uv}}{R_{vis}}\right)\xi_1[RI] + \xi_2[I_2] - K_1[R][I^*] - Q_1[RI][I^*] - Q_2[I_2][I^*] \tag{16}$$

with the laser output power density (W/cm^2) given by

$$p = -\varepsilon_\nu \Gamma_{max}\left(\frac{\pi}{2.77}\right)^{1/2} \frac{Lt_m}{\ln r_1 r_2} \tag{17}$$

where ε_ν is the photon energy and t_m is the output mirror transmission coefficient. From equations (16) and (17), the laser output clearly depends on the time-dependent composition of the gas and photodissociation rate.

Note that the recombination rate $K_1[R]$ is large compared with the parent gas quenching rate $Q_1[RI]$, and after lasing is achieved, both are small compared with the photodissociation rate of the parent gas. Early in the pump pulse, $[I_2]$ is still small so that

$$p = -\varepsilon_\nu \xi_1[RI]\left(\frac{\pi}{2.77}\right)^{1/2} \frac{Lt_m}{\ln r_1 r_2} \tag{18}$$

until late enough in the pump pulse that appreciable quenching by I_2 commences. Results for $n\text{-}C_3F_7I$ from equation (18) are shown in figure 2 in comparison with experiments (ref. 2). The experimental values shown are peak values of the quasi-CW portion of the pulse during several experimental runs and do not always correspond to times when the arc was properly focused. Also, the present calculations indicate that the detectors in reference 2 were saturated. The saturated detector response (fig. 3) was determined through calibration with a flash-lamp-pumped iodine laser. The data used to evaluate rate coefficients are based on the measured recalibration curve of the saturated detector response as shown in figure 3. The late-time CW pulse shape is then related to the processes forming I_2 and to the I_2 quenching coefficient.

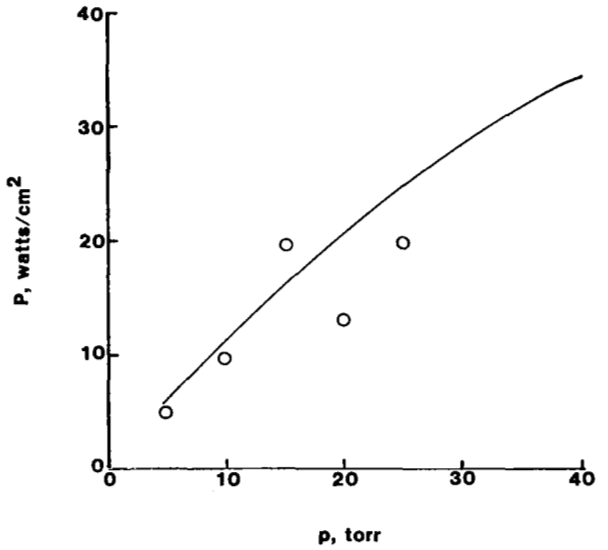

Figure 2.- Laser output intensity (eq. (18)) as a function of alkyliodide lasant pressure in comparison with experimental values taken from reference 2.

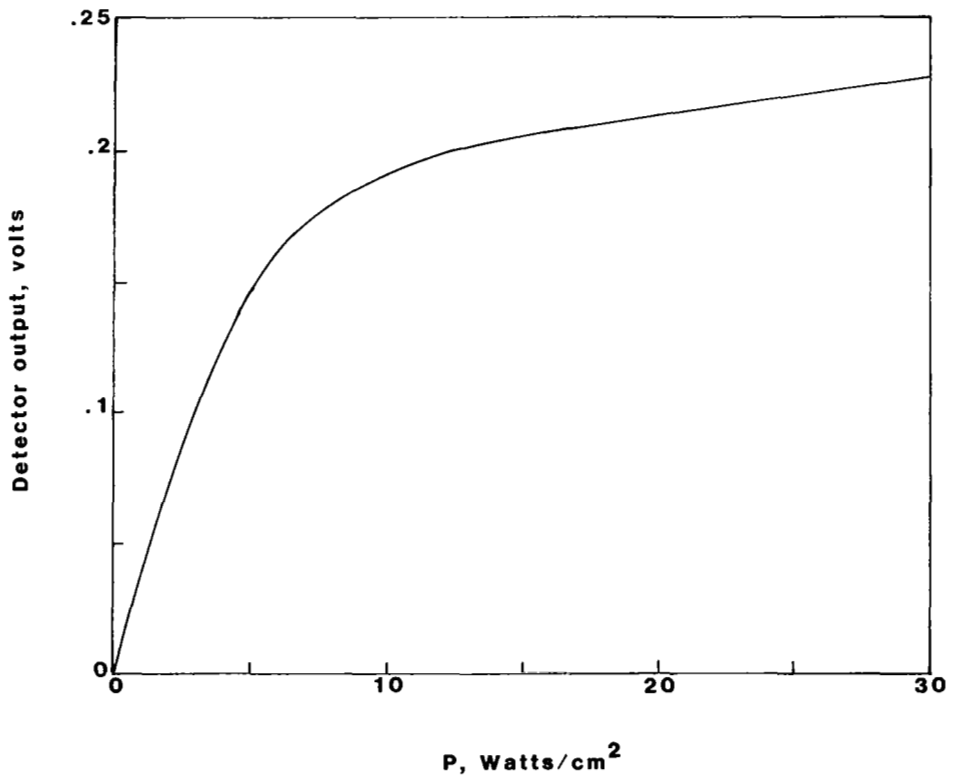

Figure 3.- Germanium detector calibration curve for the 1.3-μm iodine laser output.

When the laser is in quasi-steady-state operation, photodissociation is balanced by recombination of the ground state I with the alkyl radical to yield approximately

$$K_2[I][R] \approx \xi_1[RI] \tag{19}$$

Since the gain medium is saturated, $[R] \approx \frac{3}{2}[I]$, so that

$$[I] \approx \left(\frac{2\xi_1[RI]}{3K_2}\right)^{1/2} \tag{20}$$

Using equation (20) in equation (6) and neglecting the small terms involving C_1, C_3, and C_4, since the [RI] is large and I + I* recombination is slow, yields through integration

$$[I_2] \approx \frac{C_2}{\xi_2}[RI][I]^2\{1 - \exp[-\xi_2(t - t_{th})]\}$$

$$\approx C_2[RI][I]^2(t - t_{th}) \tag{21}$$

which is applicable for times (t) after threshold is achieved (t_{th}). Clearly from equations (20) and (21), the I_2 quenching rate is

$$q_2 \approx Q_2 \frac{C_2}{K_2} \xi_1[RI]^2(t - t_{th}) \tag{22}$$

which displays the important processes leading to the temporal variation of the late-time pulse dependence. The quantity q_2 is quite uncertain as seen from the uncertainties of Q_2, C_2, and K_2 in table II. An attempt is now made to obtain new rate coefficients and uncertainty limits from the experimental laser data.

RESULTS

A laser pulse for which the arc plasma was reasonably stationary is shown in figure 4, although motion of the arc is evident after 1.6 ms. These data are used to derive an upper bound on the late-time quenching rate q_2. For the kinetic coefficients and uncertainties for n-C_3F_7I listed in table II, the rate constant factor in equation (22) satisfies

$$1.4 \times 10^{-33} \leq \frac{Q_2C_2}{K_2} \leq 3.4 \times 10^{-30} \tag{23}$$

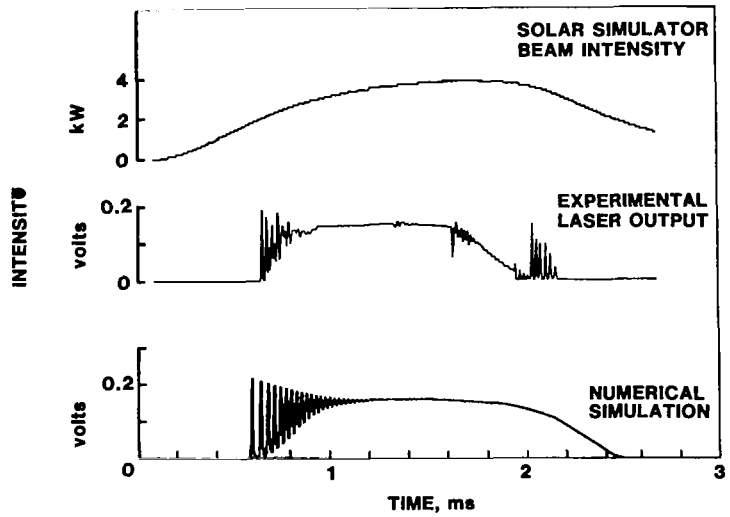

Figure 4.- Predicted germanium detector response in comparison with experimental response.

However, the present kinetic model showed the mean values of table II for Q_2, C_2, and K_2 to result in excessive quenching. New limits on these coefficients obtained from the experiments of reference 2 are shown in table III. New limits on the quenching rate factor obtained from table III are given by

$$3.8 \times 10^{-33} \leqslant \frac{Q_2 C_2}{K_2} \leqslant 1.9 \times 10^{-31} \tag{24}$$

TABLE III.- PRESENT VALUES FOR LATE-TIME KINETIC RATE COEFFICIENTS FOR $n\text{-}C_3F_7I$ IN COMPARISON WITH PREVIOUS ESTIMATES

	Present analysis	Previous published values
K_2, cm^3/s	4.3×10^{-11} $(1.9)^{\pm 1}$	8.5×10^{-11} (ref. 7) 9.0×10^{-12} (ref. 7) 7×10^{-12} (ref. 9)
Q_2, cm^3/s	3.1×10^{-11} $(1.6)^{\pm 1}$	5×10^{-12} (ref. 15) 3.2×10^{-12} (ref. 6) 2.1×10^{-11} (ref. 16) $(3.1 \pm 0.5) \times 10^{-11}$ (refs. 8, 17-19)
C_2, cm^6/s	3.7×10^{-32} $(2.3)^{\pm 1}$	8.5×10^{-32} (ref. 7)

The calculated germanium detector response to the theoretical laser output for the kinetic rates $K_2 = 2.3 \times 10^{-11}$, $Q_2 = 4.4 \times 10^{-11}$, and $C_2 = 6.9 \times 10^{-32}$ is shown in figure 4 in comparison with the experimental detector response. Note that because the image of the arc was offset from the laser tube axes, only 40-percent power levels were achieved. Also shown in table III are kinetic rate coefficients associated with other experiments which are clearly inconsistent with the present results. In particular, the present value of K_2 lies midway between the previously reported values which differed by an order of magnitude. The earlier values of Q_2 (refs. 6 and 15) differ from the present results, while more recent work (refs. 8 and 16 to 19) is consistent with our results. Although the $n\text{-}C_3F_7I$ stabilized I + I recombination coefficient found by Kuznetsova and Maslov (ref. 7) is consistent with the present value of C_2, much lower values cannot be ruled out by the present analysis.

Langley Research Center
National Aeronautics and Space Administration
Hampton, VA 23665
June 14, 1983

REFERENCES

1. Wilson, J. W.; and Lee, J. H.: Modeling of a Solar-Pumped Iodine Laser. Virginia J. Sci., vol. 31, no. 3, Fall 1980, pp. 34-38.

2. Lee, Ja H.; and Weaver, W. R.: A Solar Simulator-Pumped Atomic Iodine Laser. Appl. Phys. Lett., vol. 39, no. 2, July 15, 1981, pp. 137-139.

3. Koffend, J. Brooke; and Leone, Stephen R.: Tunable Laser Photodissociation: Quantum Yield of $I^*(^2P_{1/2})$ From CH_2I_2. Chem. Phys. Lett., vol. 81, no. 1, July 1, 1981, pp. 136-141.

4. Leone, Stephen R.: Molecular Photofragmentation Processes Related to Solar-Pumped Gas Laser Development. NASA CR-169408, 1982.

5. Wilson, Kent R.: Photofragment Spectroscopy of Dissociative Excited States. Excited State Chemistry, James N. Pitts, ed., Gordon & Breach, Science Pub., Inc., c.1970, pp. 33-58.

6. Turner, C. E., Jr.; and Rapagnani, N. L.: Kinetic Modeling of Photodissociation Iodine Laser Amplifiers. UCID-16935 (Contract No. W-7405-Eng-48), Lawrence Livermore Lab., Univ. of California, Oct. 23, 1974.

7. Kuznetsova, S. V.; and Maslov, A. I.: Investigation of the Reactions of Atomic Iodine in Photodissociation Laser Using $n\text{-}C_3F_7I$ and $i\text{-}C_3F_7I$ Molecules. Soviet J. Quantum Electron., vol. 3, no. 6, May-June 1974, pp. 468-471.

8. Beverly, R. E., III; and Wong, M. C.: Transverse-Discharge Excitation of the 1.315-μm Atomic Iodine Laser II. Kinetic Model. Opt. Commun., vol. 20, no. 1, Jan. 1977, pp. 23-28.

9. Kuznetsova, S. V.; and Maslov, A. I.: New Reaction Rate Constants of CF_3, $n\text{-}C_3F_7$, and $i\text{-}C_3F_7$ Radicals. Soviet J. Quantum Electron., vol. 8, no. 7, July 1978, pp. 906-909.

10. Skorobogatov, G. A.; and Slesar, O. N.: Measurement of the Absolute Rate Constants of the Gas-Phase Recombination Reactions of Fluorocarbon Radicals With Themselves and With Iodine Atoms. Vestn. Leningr. Univ. Fiz. Khim., vol. 4, no. 1, 1979, pp. 39-45.

11. Skorobogatov, G. A.; Komarov, V. S.; and Seleznev, V. G.: Absolute-Photometry Determination of the Rate Constant of the Gas-Phase Reaction of the Radical Compound C_3F_7 and $I(^2P_{3/2})$. Soviet Phys. - Tech. Phys., vol. 19, no. 9, Mar. 1975, pp. 1239-1241.

12. Fisk, George A.: The Effects of Chemical Kinetics and Starting Material Regeneration on the Efficiency of an Iodine Laser Amplifier. Rep. SAND77-0880, Sandia Labs., May 1977.

13. Hohla, Kristian; and Kompa, Karl L.: The Photochemical Iodine Laser. Handbook of Chemical Lasers, R. W. F. Gross and J. F. Bott, eds., John Wiley & Sons, Inc., 1976, pp. 667-701.

14. Stephan, K.-H.; and Comes, F. J.: Chemiluminescent Iodine Atom Recombination. Chem. Phys. Lett., vol. 65, no. 2, Aug. 15, 1979, pp. 251-256.

15. Donovan, R. J.; and Husain, D.: Spin Orbit Relaxation of Metastable Iodine Atoms. Nature, vol. 206, no. 4980, Apr. 10, 1965, pp. 171-173.

16. Kartazaev, V. A.; Penkin, N. P.; and Tolmachev, Yu. A.: Determination of the Temperature Dependence of the Rate Constant Representing Quenching of Metastable Iodine Atoms by Iodine Molecules. Soviet J. Quantum Electron., vol. 7, no. 5, May 1977, pp. 608-610.

17. Busch, George E.: Kinetic Analyses of Energy Storage in a Chemically Pumped Iodine Laser. IEEE J. Quantum Electron., vol. QE-17, no. 6, June 1981, pp. 1128-1133.

18. Arnold, I.; Comes, F. J.; and Pointech, S.: Laser Induced Photodissociation of Iodine Molecules Spin-Orbit Relaxation of $I(^2P_{1/2})$. Chem. Phys., vol. 9, no. 1-2, June 1975, pp. 237-240.

19. Hofmann, Hubert; and Leone, Stephen R.: Quenching and Reactions of Laser-Excited $I(5^2P_{1/2})$ Atoms With Halogen and Interhalogen Molecules. J. Chem. Phys., vol. 69, no. 2, July 15, 1978, pp. 641-646.

20. Bunker, Don L.; and Davidson, Norman: A Further Study of the Flash Photolysis of Iodine. J. American Chem. Soc., vol. 80, no. 19, Oct. 5, 1958, pp. 5085-5090.

21. Blake, J. A.; and Burns, George: Kinetics of Iodine Atom Recombination Between 300° and 1164°K. J. Chem. Phys., vol. 54, no. 4, Feb. 15, 1971, pp. 1480-1486.

22. Lengyel, Bela A.: Introduction to Laser Physics. John Wiley & Sons, Inc., c.1966.

SYMBOLS

A	Einstein coefficient of spontaneous emission, s^{-1}
c	velocity of light, cm/s
$C(r,\ell)$	solar-simulator intensity of illumination, kW/cm^2
C_o	peak solar-simulator intensity, kW/cm^2
C_1	RI stabilized I + I* recombination rate coefficient, cm^6/s
C_2	RI stabilized I + I recombination rate coefficient, cm^6/s
C_3	I_2 stabilized I + I* recombination rate coefficient, cm^6/s
C_4	I_2 stabilized I + I recombination rate coefficient, cm^6/s
D_o	photoabsorption line width, nm
f	fractional absorption near line center
g	oscillator cavity coupling coefficient
$[I]$	atomic iodine density, cm^{-3}
$[I_2]$	molecular iodine density, cm^{-3}
$[I^*]$	electronically excited atomic iodine density, cm^{-3}
K_1	R + I* recombination rate coefficient, cm^3/s
K_2	R + I recombination rate coefficient, cm^3/s
K_3	R + R recombination rate coefficient, cm^3/s
L	lamp image length parameter, cm
L_c	distance between laser end mirrors, cm
p	alkyliodide partial pressure at room temperature, torr
P	laser output power density, W/cm^2
Q_1	I* quenching coefficient for RI, cm^3/s
Q_2	I* quenching coefficient for I_2, cm^3/s
r,ℓ	cylindrical coordinates of the lamp image, cm
r_b	laser beam width parameter, cm
r_1,r_2	combined reflection coefficients of the Brewster window and end mirror at each end of the laser tube

R	lamp image width parameter, cm
$[R]$	alkyl radical density, cm^{-3}
$[R_2]$	alkyl dimer density, cm^{-3}
$[RI]$	alkyliodide density, cm^{-3}
R_{uv}, R_{vis}	ultraviolet and visible light reflection coefficients for the MgF_2-coated aluminum cone
S_i	maximum photodissociation rate of the ith chemical species, s^{-1}
t	time, s
t_m	output mirror transmission coefficient
x	penetration distance into the lasant gas, cm
Γ_{max}	stimulated emission rate at the spatial peak of the light pulse, cm^{-3}-s^{-1}
ε_ν	radiation energy quantum from the I*, eV
λ_o	central wavelength for photoabsorption, nm
ξ_i	photodissociation rate of ith chemical species at a depth x of penetration
ρ	photon density in resonance with the optical cavity, cm^{-3}
σ	stimulated emission cross section, cm^2
σ_o	photoabsorption cross section at the central frequency, cm^{-1}-$torr^{-1}$
τ_c	optical cavity time constant, s
ϕ_{I*}	quantum yield for excited iodine

1. Report No.	2. Government Accession No.	3. Recipient's Catalog No.
NASA TP-2182		

4. Title and Subtitle	5. Report Date
SOLAR-SIMULATOR-PUMPED ATOMIC IODINE LASER KINETICS	August 1983
	6. Performing Organization Code 506-55-13-01

7. Author(s)	8. Performing Organization Report No.
John W. Wilson, S. Raju, and Y. J. Shiu	L-15615
	10. Work Unit No.

9. Performing Organization Name and Address	11. Contract or Grant No.
NASA Langley Research Center Hampton, VA 23665	
	13. Type of Report and Period Covered: Technical Paper

12. Sponsoring Agency Name and Address	14. Sponsoring Agency Code
National Aeronautics and Space Administration Washington, DC 20546	

15. Supplementary Notes

John W. Wilson: Langley Research Center.
S. Raju and Y. J. Shiu: Hampton Institute, Hampton, Virginia. Work performed under NASA Grant NSG-1595.

16. Abstract

The literature contains broad ranges of disagreement in kinetic data for the atomic iodine laser. A kinetic model of a solar-simulator-pumped iodine laser is used to select those kinetic data consistent with recent laser experiments at the Langley Research Center. Analysis of the solar-simulator-pumped laser experiments resulted in the following estimates of rate coefficients: for alkyl radical ($n\text{-}C_3F_7$) and atomic iodine (I) recombination, 4.3×10^{-11} $(1.9)^{\pm 1}$ cm^3/s; for $n\text{-}C_3F_7I$ stabilized atomic iodine recombination (I + I) 3.7×10^{-32} $(2.3)^{\pm 1}$ cm^6/s; and for molecular iodine (I_2) quenching, 3.1×10^{-11} $(1.6)^{\pm 1}$ cm^3/s. These rates are consistent with the recent measurements.

17. Key Words (Suggested by Author(s))	18. Distribution Statement
Lasers Energy conversion Solar simulator Photochemical	Unclassified - Unlimited Subject Category 36

19. Security Classif. (of this report)	20. Security Classif. (of this page)	21. No. of Pages	22. Price
Unclassified	Unclassified	15	A02

For sale by the National Technical Information Service, Springfield, Virginia 22161

NASA-Langley, 1983

6 1 1U,D, 830810 S00903DS
DEPT OF THE AIR FORCE
AF WEAPONS LABORATORY
ATTN: TECHNICAL LIBRARY (SUL)
KIRTLAND AFB NM 87117